


3D Data Processing to Characterize the Spatial Variability of Sugarcane Fields

Tatiana Fernanda Canata¹  · Maurício Martello¹ · Leonardo Felipe Maldaner¹ · Jadir de Souza Moreira² · José Paulo Molin¹

Received: 21 April 2021 / Accepted: 25 August 2021 / Published online: 9 September 2021
© Society for Sugar Research & Promotion 2021

Abstract The adoption of precision agriculture involves a demand for equipment and solutions to create an accurate diagnostic of the spatial variability to be managed at the field level. Sugarcane has faced some challenges due to the limited solutions adapted to the crop, which develops throughout the year and involving a large-scale harvest. LiDAR (Light Detection and Ranging) technology is a high-resolution tool that permits the measurement of vegetative growth in a non-destructive way, assisting, for example, in harvest planning. The objective was to describe the three-dimensional (3D) data processing to characterize the spatial variability of sugarcane fields in the pre-harvest period. An aerial platform was used for data acquisition 10 days before and after harvesting. The digital models of surface, of terrain, and the canopy height model (CHM) were generated to spatialize plants height based on point cloud. The LiDAR-derived metrics extracted were percentiles (P50th; P90th–P99th), with the highest value of the coefficient of variation observed for the P50th (59%), indicating that there is high spatial variability in plant height. The RMSE (Root Mean Squared Error) among field measurements and sugarcane stalk height from CHM was 0.47 m. This study demonstrates that 3D sensing data can provide relevant information for the assessment of the crop height and, potentially, to consider it as an indicator of the field regions with distinct levels of production.

Keywords Precision agriculture · Point clouds · Remote sensing · Site-specific

Introduction

The application of remote sensing (RS) techniques in agriculture allows for the collection of high-resolution data (spatial and temporal) for mapping and monitoring crops, which are essential to the PA practices. RS allows for the identification of agronomic factors associated with the inherent variability of the fields (Molin et al. 2015). Both aerial images and scanning sensors (laser, ultrasonic, and radar) have been adopted to detect the spatial variability of agricultural fields and to support agricultural management decisions. The main reason is the capacity of the embedded sensors on platforms to obtain a high sample density, in shorter time, and large-scale (Buelvas et al. 2019). Maes and Steppe (2019) reported the progress of applying RS tools to the PA scenario as a solution to provide detailed spatial information to the agronomical diagnostics. Some examples regarding the potential of the image-based aerial platforms are assessing drought stress in early stages, to develop site-specific weed detection, to detect growth vigor, crop nutrient status, and yield prediction. The authors highlighted the integration of different datasets to improve the applicability of the developed models. The goal is to optimize agricultural practices by increasing the systems knowledge due to increased availability and quality of agronomic data (Saiz-Rubio and Rovira-Más 2020).

The agricultural applications considering laser sensors, a LiDAR technology, started in silviculture during the 1960s to estimate forest biomass, such as eucalyptus (Ross,

✉ Tatiana Fernanda Canata
tatiana.canata@usp.br

¹ Department of Biosystems Engineering, “Luiz de Queiroz” College of Agriculture (ESALQ), University of Sao Paulo (USP), 11 Padua Dias Avenue, Piracicaba 13418-900, Brazil

² Expert Aerial Industrial Services (SAI), 579 Afonso Braz Street, São Paulo 04511-011, Brazil

2013). Silva et al. (2020) demonstrated the potential of modeling forest plantations using LiDAR and field data (stem volume). Other agricultural research studies utilized 3D point clouds to characterize the structure of perennial crops (Jiang et al. 2019; Murray et al. 2020), the modeling of orange orchards (Colaço et al. 2019), the estimation of barley, paddy rice, and wheat biomass (Brocks and Bareth et al. 2018; Tilly et al. 2015; Walter et al. 2019), the assessment of wheat nitrogen status (Eitel et al. 2014), the measurement of dry matter yield of forage (Gebremedhin et al. 2019), and the analysis of plant growth within-field (Escolà et al. 2016; Sun et al. 2018), among others. Paulus et al. (2014) verified the response of the volumetric shape of sugar beet subject to drought conditions based on laser sensors as a potential technique for plant phenotyping. Paulus (2019) introduced different measuring techniques using LiDAR for crop analysis and suggested to advance on the automated extraction of the attributes related to the crop yield from point clouds. Another approach is the integration of laser sensors and reflectance data to infer about crop biomass (Okhrimenko et al. 2019; Tilly et al. 2015). Other agricultural applications have been supported by 3D sensing data, such as fruit detection for apple orchards with an accuracy of more than 80% (Gené-Mola et al. 2020). Three-dimensional sensing data are commonly collected through aerial or terrestrial platforms which are referred to as aerial laser scanning (ALS) and terrestrial laser scanning (TLS), respectively. Both platforms have been used in agriculture to provide crop canopy models along the development cycle of the crop and integrated to calibrate structural attributes of the plants (Bazewew et al. 2018; Hopkinson et al. 2013). Li et al. (2017) investigated the potential of point clouds generated from ALS to characterize the structural complexity of maize canopy, such as leaf area index estimation with a relative error of 5.63%.

The use of unmanned aerial vehicle (UAV) has been a low-cost alternative to monitor crops compared to the LiDAR systems. Mesas-Carrascosa et al. (2020) developed a solution for viticulture-based utilizing an RGB sensor mounted on a UAV to derive crop canopy information, such as the heights of individual grapevines with an error of 0.07 m. Maimaitijiang et al. (2020) proposed a method to model and predict soybean yields from UAV and data fusion as an alternative to the field management. The main limitations of this approach are the reduced payload of the platform, a lack of sensors able to deal with the spectral saturation effect, the independence of the ambient light conditions, and difficulties related to the signal penetration of the dense crop canopy prior to the harvest period (Deery et al. 2014; Poley and McDermid, 2020). Shendryk et al. (2020) used multirotor UAV with LiDAR and imaging sensors embedded for prediction of biomass and leaf nitrogen content in sugarcane; they found moderate

relationship ($R^2 \leq 0.52$) to estimate sugarcane biomass based on 3D modeling and multispectral images.

Sugarcane plays an important role in the Brazilian agricultural economy. Brazil is the largest producer of sugarcane in the world market (about 9.0 M ha) and the first in the production of sugar and ethanol (CONAB, 2020). The high demand regarding domestic and foreign markets for products obtained through sugarcane, and the expansion of production areas in different regions of the country have intensified the need to obtain information that has a direct relationship with sugarcane yield. Mapping sugarcane areas using multi-temporal data has been discussed to monitor spatial variability of the fields based on orbital images (Luciano et al. 2018; Wang et al. 2019). Also, the spectral bands (reflectance data and vegetation indices) have been investigated for sugarcane yield forecasting (Bégué et al. 2010; Rahman and Robson 2020).

Despite the potential to explore and model agronomic data from low-cost images, the problems associated with the spectral saturation effect prior to the harvest, and also selecting the most appropriate period to collect the data to determine crop yield are the main challenges limiting to implementation of these methods for high biomass crops (e.g., maize, sugarcane, and wheat). Molijn et al. (2018) proposed a methodology for estimating sugarcane biomass from soil reference data and orbital images, associating biometric measurements, to monitor the dynamics of the sugarcane production. Canata et al. (2019) developed a measurement system based on TLS as a spatial assessment of sugarcane plant height in the pre-harvest period. To advance the understanding and application of LiDAR technology in sugarcane, the objective of this paper is to describe the techniques of 3D data processing for mapping the spatial variability of sugarcane fields. A validation of the LiDAR measurements is also described.

Material and Methods

Study Site

The study was conducted in a 36.05 ha commercial sugarcane area with three fields, located near Botucatu, São Paulo, Brazil (22° 41' 42.8" S; 48° 16' 54.0" W; elevation 480 m) for the 2018/2019 sugarcane growing season. The climate in the region of study is mesothermal, Cwa, i.e., humid subtropical including drought in the winter (from June to September) and rain from November to April, and the average annual rainfall in that municipality is 1433 mm. The average air relative humidity is 71% with an annual average temperature of 23°C (Cunha and Martins 2009). The sugarcane variety SP83-2847 (4th ratoon) was planted with a row spacing of 1.5 m on an Argisol soil for

all study sites. All fields were mechanically harvested green late in the season (wet time of the year—November).

Data Acquisition and Processing

To investigate the application of LiDAR technology for mapping the variation of sugarcane plant heights, the following embedded and integrated equipment was used: a laser sensor ALTM Gemini 56,100 (OPTECH), an inertial unit, and a GNSS (Global Navigation Satellite Systems) receiver mounted on a helicopter. The sensors were mounted at a nadir angle with scans over the sugarcane fields. The average flying altitude was 500 m above ground level. The main specifications of the data acquisition are shown in Fig. 1. The data acquisition occurred on two occasions, within each collection time, and manual measurements were taken immediately after the ALS data acquisition. The first data acquisition (first flight) was carried out 10 days before harvesting for the three fields selected according to the validation points. The second flight occurred 10 days after harvesting with the same equipment to create the DTM of reference.

The planimetric coordinates (X and Y) and the ellipsoid height values (Z) were computed for all laser sensor data (points) and georeferenced using the post-processing method. The original point clouds were stored in LAS format and projected on the WGS84/UTM22S coordinate system. The preliminary analyzes of the point clouds were done using CloudCompare 2.10.2 software (Girardeau-

Montaut). All data allocate outside the field boundary and outliers were manually excluded from point clouds.

The function *grid_metrics* of the *lidR* package (Roussel et al. 2019) from R statistical software (R Core Team, 2017) was used to create the DSM. *lidR* package is considered an interface for data manipulation and visualization of airborne LiDAR data. The *grid_metrics* function is an area-based approach. In the first data acquisition, the 3D data was used to calculate the DSM, which is the absolute height of sugarcane plants. The data processing steps to generate the DSM were (i) to consider the maximum elevation parameter of the filtered point cloud generated before harvesting; (ii) to rasterize the data with a pixel resolution of 0.5 m, due to the row spacing of sugarcane plants, and the recommendation of Mielcarek et al. (2020); (iii) computing the metrics for each cell. The same function was used to generate the percentiles (P50th; from P90th to P99th) that are common LiDAR-derived metrics calculated in studies of 3D data (Gorgens et al. 2017; Li et al. 2017). Eleven metrics were considered to support the identification of the spatial variability in sugarcane fields. The DTMs for both point clouds (before and after harvesting) were generated using the function *grid_terrain* of *lidR* package (Roussel et al. 2019) from R statistical software (R Core Team 2018). Only LiDAR points classified as ground (classification = 2, according to LAS file format) were interpolated using triangulated irregular network (TIN), Delaunay triangulation method, with the same pixel resolution of DSM (0.5 m). The relationship between the

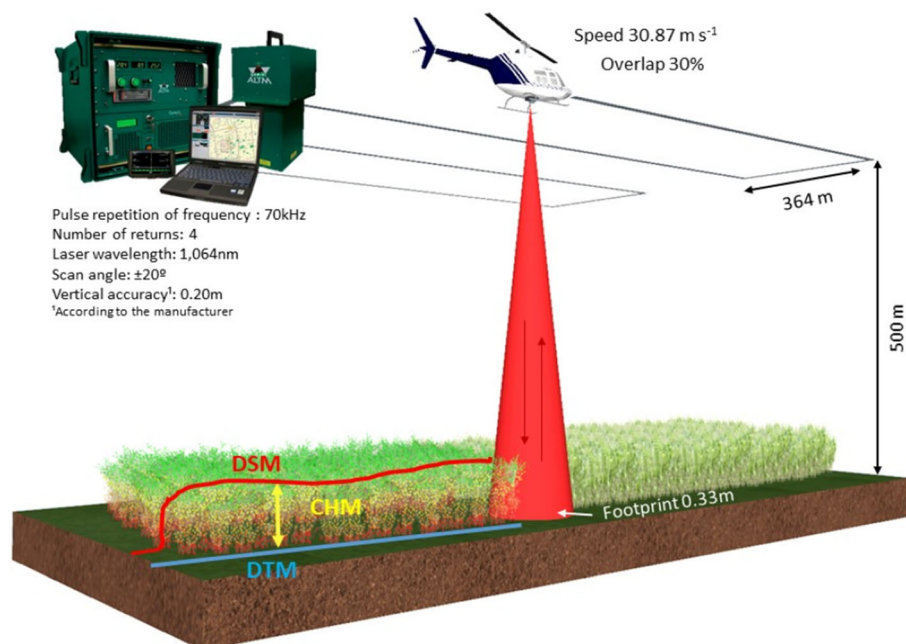


Fig. 1 Overview of the LiDAR data acquisition from airborne laser scanning

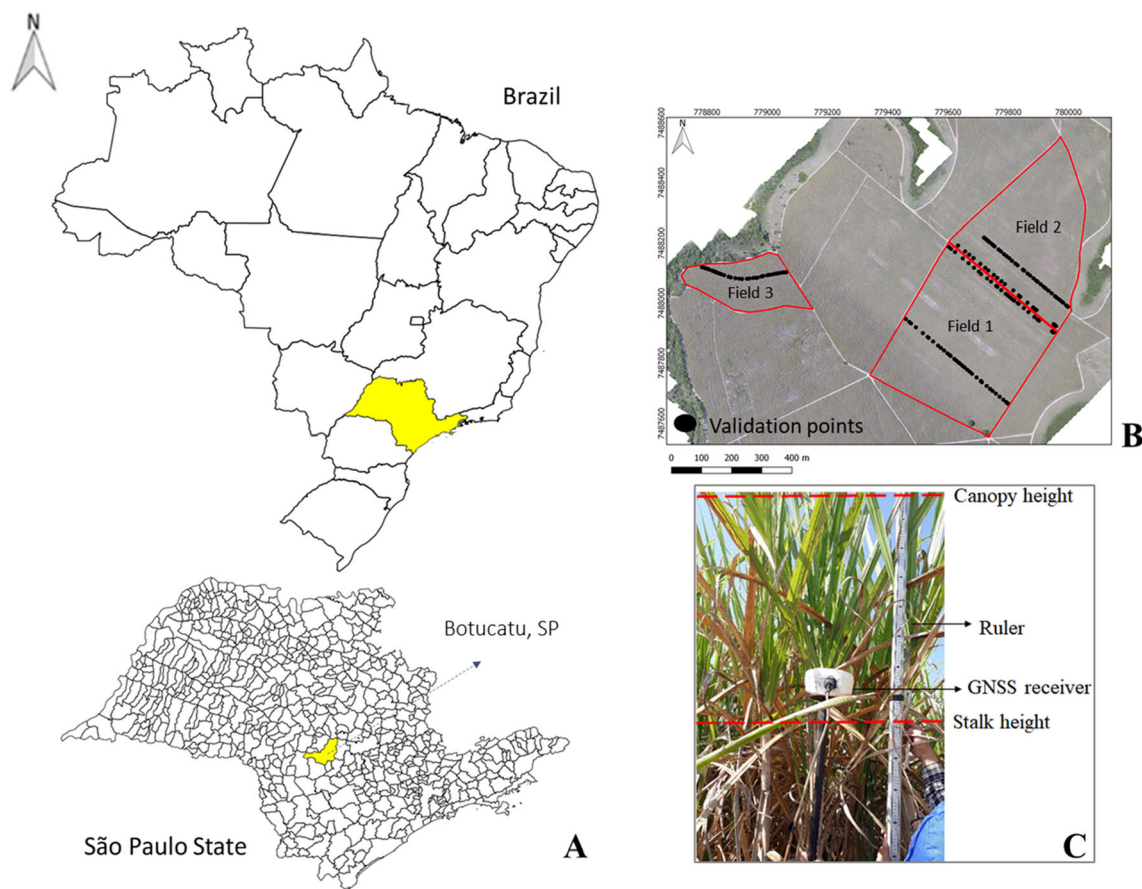


Fig. 2 Sugarcane study site (a); validation points (b); field measurements (c)

elevation values from both DTMs was evaluated by calculating the RMSE according to Eq. (1).

$$\text{RMSE} = \sqrt{\frac{1}{n} \sum_{i=1}^n (z_i - z)^2} \quad (1)$$

where n is the number of the sample, z_i is the predicted height, and z is the observed height.

Determining the crop canopy height with LiDAR requires an estimation of the ground level and subtracting it from the absolute height of the elevation (Eq. 2, Jimenez-Berni et al. 2018; Loudermilk et al. 2009). The DTM can be obtained from a scan with bare soil, while the crop surface model is calculated from the top-most points of the point cloud, using a selection based on the top percentile (Friedli et al. 2016; Hämmerle and Höfle, 2014). The purpose of the data acquisition after harvesting was to map the DTM of reference.

$$\text{CHM} = \text{DSM} - \text{DTM} \quad (2)$$

where CHM is the canopy height model (m); DSM is the digital surface model (m); DTM is the digital terrain model (m).

Field Data Collection

Manual measurements were collected across three fields (Field 1—18.07 ha; Field 2—12.67 ha; Field 3—5.31 ha) as harvesting front advanced. Totally 162 validation points were allocated on the study site (Fig. 2a), and the geographical coordinates for each one were recorded using a GNSS receiver with satellite differential correction (Fig. 2b). The sugarcane stalk height and the canopy height (the highest leaf of the plant) were measured and georeferenced using a ruler (Fig. 2c), according to the methodology described by Portz et al. (2012). For measuring the stalk height, we considered the top visible dewlap leaf as reference (stem distance from the ground level). The accuracy of the plant height measurements was assessed by calculating the RMSE. In addition, linear regression analysis was used to describe the relationship among plant height estimation from CHM and field measurements. The coefficient of determination (R^2) was calculated as a measure of the goodness of fit from the prediction model. The linear regression was used to develop equations that relate LiDAR-derived metrics with reference data (field measurements) (Mielcarek et al. 2018).

The CHM and the percentiles from point cloud were converted to vector layer on quantum geographic information system (QGIS 2.18.26, QGIS Development Team 2018) and compared with the georeferenced field measurements. The relationship among LiDAR and field data has been used to verify the relative error of measuring plant height (Borra-Serrano et al. 2019; Harkel et al. 2020), considering it an indicator of yield and highly influenced by soil, temperature, and light intensity (Cholula et al. 2020). The main steps and the computational tools for processing 3D sensing data are shown in Fig. 3. The spatial variability was determined according to the descriptive statistics of the dataset and the criteria established by Gomes and Garcia (2002), considering the coefficient of variation (CV). This criterion is useful for PA as an initial analysis to identify the within-field regions with a distinct potential of production (Molin et al. 2015). All statistical analyses were conducted in R statistical software (R Core Team 2018).

Results and Discussion

Point Clouds Assessment

3D sensing data demonstrates the common characteristic of high-resolution data (about 13 points m⁻²) for the point clouds generated before and after harvesting for the selected fields. The descriptive statistics for both point

clouds, considering the preliminary data filtering, is shown in Table 1.

The point cloud generated before harvesting for the selected field (Field 1) is shown in Fig. 4. Each point represents the positioning (X, Y) and the elevation (Z) in the same coordinate system. Considering all fields, an average point density of 14 points m⁻² was obtained for the data acquisition performed before harvesting. 35% of the total points were classified as ground for the first data acquisition.

It was observed that the overlap from ALS influenced on digital models due to the density of points; thus a normalization of the elevation values was performed. Crop mapping using ALS provides a more detailed characterization of the plant profile due to the multiple pulses emitted by the laser sensor and enables the data acquisition for large-scale and shorter time. Also, the data acquisition from ALS is unlimited by the availability of crop inter-row at the field. Jimenez-Berni et al. (2018) described LiDAR as a direct measurement of the crop canopy height that allows a multi-temporal and non-destructive assessment of ground cover and above-ground biomass of wheat. Also, point cloud has been considered a technique that provides more robust dataset to guide agronomic interventions. Colaço et al. (2018) discussed the potential application of high-resolution 3D modeling for precision horticulture according to the volume variability of tree canopies.

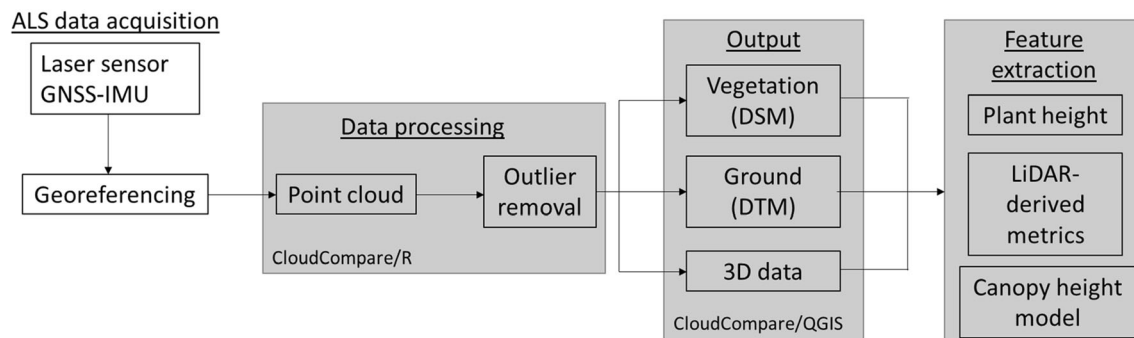


Fig. 3 Schematic of the LiDAR data acquisition and data processing workflow

Table 1 Descriptive statistics of the point clouds considering all fields

Point cloud	<i>n</i>	Density points m ⁻²	Minimum Elevation (m)	Maximum	Mean	Median	SD	CV (%)
Before harvesting	4,895,596	13.60	459.19	505.77	474.88	474.98	4.61	0.97
After harvesting	4,684,655	13.01	459.29	495.88	474.29	474.27	4.20	0.88

n—number of samples, *SD*—standard deviation, *CV*—coefficient of variation

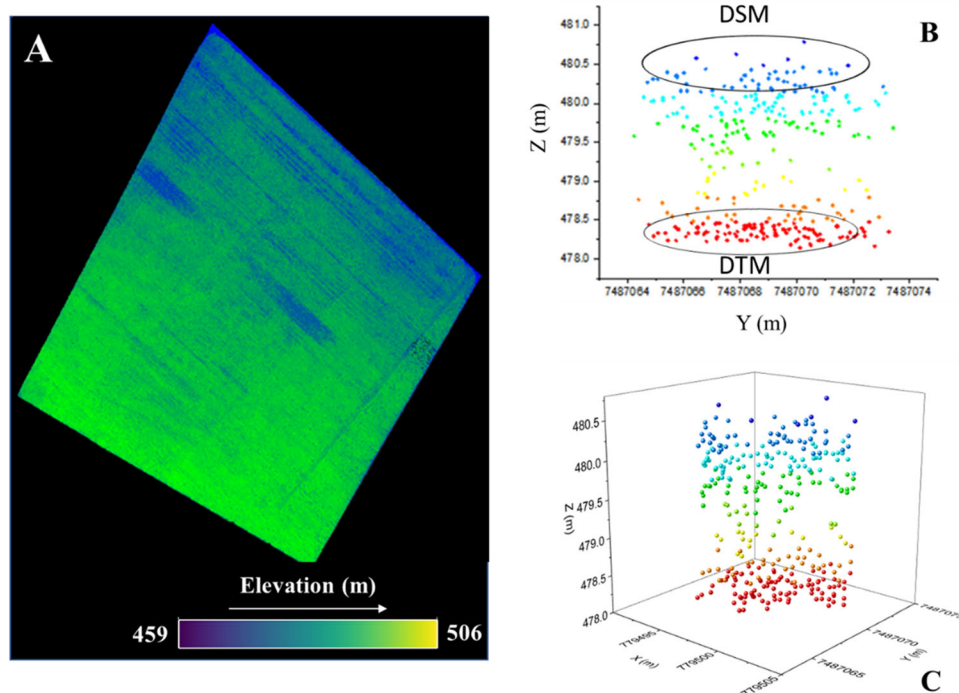


Fig. 4 Point cloud generated before harvesting (a); representation of a point cloud section: 2D (b); 3D (c)

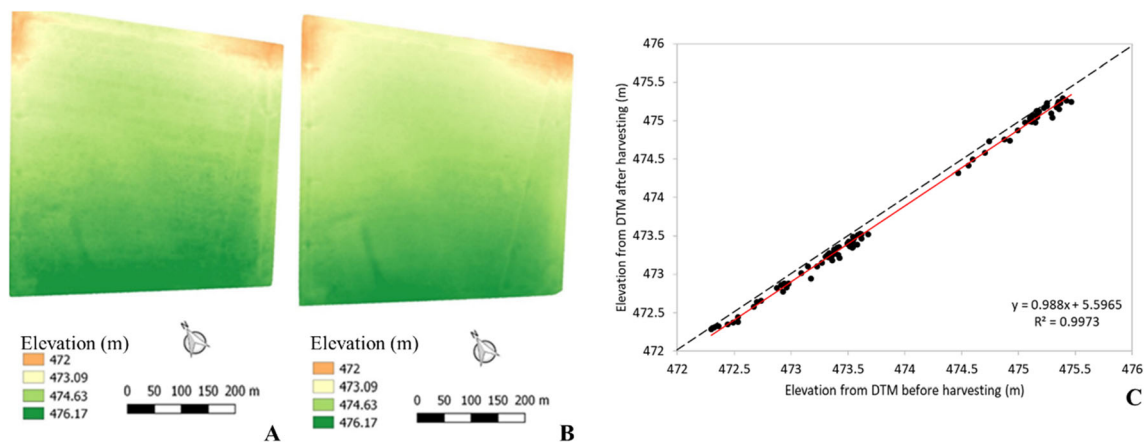


Fig. 5 Digital terrain models for before harvesting (a); and after harvesting (b); Relationship between both digital terrain models (c). The dashed line represents the 1:1 line and the solid line represents the fitted linear function

Digital Terrain Models

The point density achieved was sufficient to generate the DTM (Fig. 5a) for the first data acquisition, which had a similar distribution of the elevation values from DTM after harvesting (Fig. 5b). The relationship between both DTMs for one field (Field 1) is shown in Fig. 5c, demonstrating that the linear regression provided an accuracy of $R^2 = 0.997$ and RMSE of 0.13 m.

The settings adopted for the data acquisition by an ALS enabled the detection of ground points in a condition of

sugarcane pre-harvest period (high-density distribution of the plants and overlapping leaves). This result was obtained for the specific field conditions found on the period of the data acquisition, and other field conditions should be investigated to verify if a single flight is sufficient to generate the DTM. Hämmerle and Höfle (2014) reported the effect of reduced point density of laser sensor data on generating digital models for grain crop fields. They found that the accurate measurement of the crop height did not always improve with increasing on point density. Other studies also related the effect of point density reduction on

Table 2 Descriptive statistics of the validation points for each field

	Field	n	Minimum	Maximum	Mean	Median	SD	RMSE	CV (%)
Stalk height (m)	1	63	1.34	2.52	1.87	1.86	0.26	0.62	13.90
	2	62	1.20	2.90	2.07	2.09	0.41	0.51	19.80
	3	37	1.57	2.71	2.07	2.06	0.27	0.47	13.04
Canopy height (m)	1	63	2.59	4.10	3.22	3.12	0.34	0.81	10.56
	2	62	2.44	4.30	3.70	3.10	0.41	0.70	11.08
	3	37	2.61	3.90	3.17	3.20	0.29	0.72	9.14
CHM (m)	1	63	1.80	3.09	2.45	2.44	0.28	–	11.43
	2	62	1.57	3.23	2.47	2.57	0.37	–	14.98
	3	37	1.44	3.03	2.48	2.53	0.32	–	12.90

CHM—canopy height model, n—number of samples, SD—standard deviation, RMSE—root mean squared error, CV—coefficient of variation

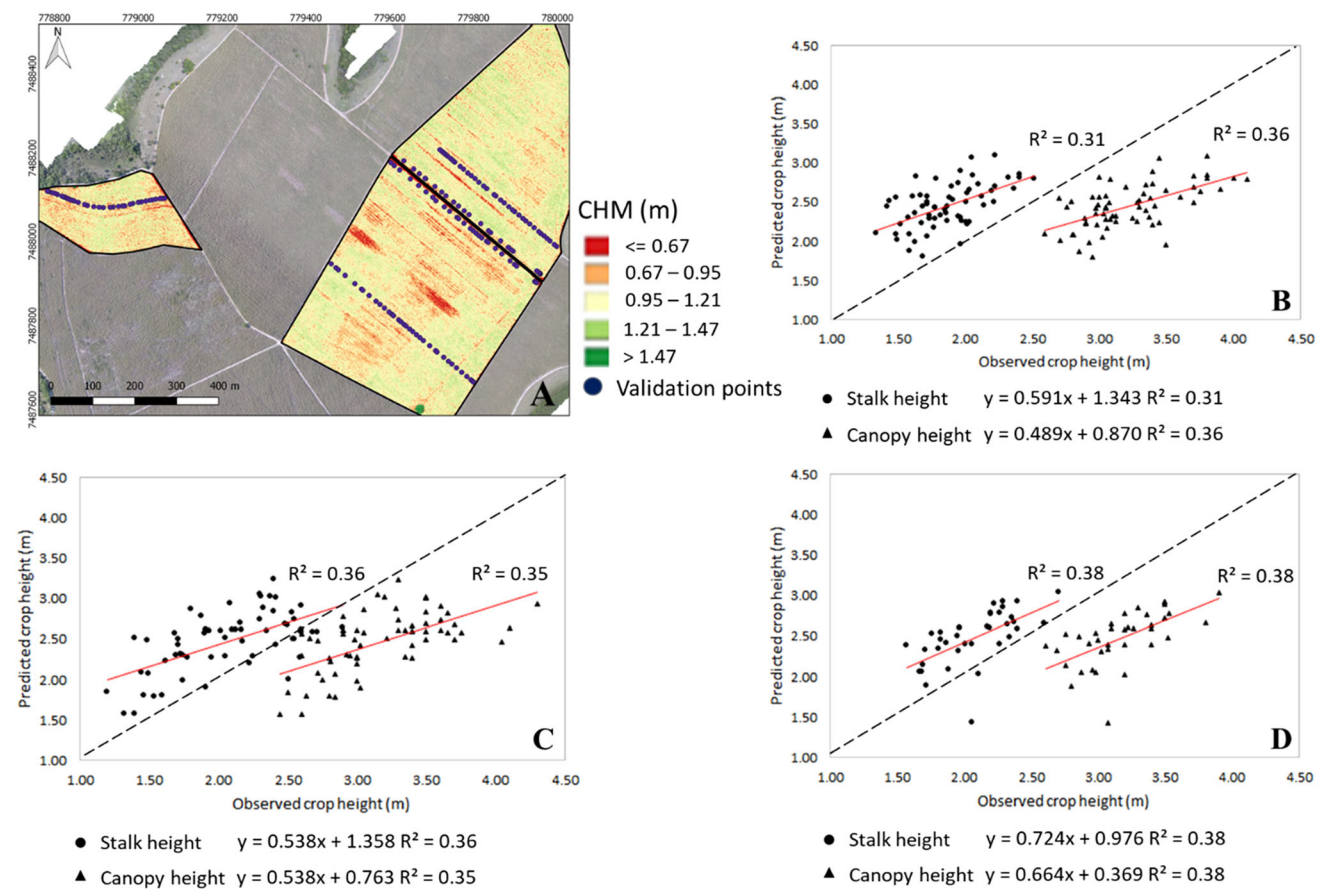


Fig. 6 Canopy height model (a); Relationship between the validation points and predicted values from CHM for field 1 (b); field 2 (c); field 3 (d). The dashed line represents the 1:1 line and the solid line represents the fitted linear function

digital models as a parameter to help choose the settings for the data acquisition (Luo et al. 2016; Silva et al. 2017).

Comparing 3D Data and Field Measurements

The descriptive statistics of the validation points (Table 2) showed that the minimum sugarcane stalk height and crop

canopy height were 1.20 m and 2.44 m, respectively. The maximum values were of 2.90 m and 4.30 m, respectively. The CV values indicated that there was a greater variability of the stalk height (19%) in relation to the crop canopy height (9%). Considering all fields, the RMSE between the laser sensor data and the field data ranged from 0.47 to 0.62 m for stalk height, and from 0.70 to 0.81 m for crop

Table 3 Descriptive statistics of the LiDAR-derived metrics

	Field	Plant height (m)										
		P50*	P90*	P91*	P92*	P93*	P94*	P95*	P96*	P97*	P98*	P99*
Minimum	1	0	0	0	0	0	0	0	0	0	0	0
	2	0	0	0	0	0	0	0	0	0	0	0
	3	0.08	0.08	0.08	0.08	0.08	0.08	0.08	0.08	0.08	0.08	0.08
Maximum	1	2.70	2.70	2.70	2.70	2.70	2.70	2.70	2.70	2.70	2.70	2.70
	2	2.51	2.70	2.70	2.71	2.71	2.72	2.72	2.73	2.75	2.78	2.81
	3	2.88	2.95	2.95	2.96	2.96	2.96	2.96	2.97	2.97	2.97	2.97
Mean	1	1.41	1.65	1.65	1.66	1.66	1.67	1.67	1.68	1.78	1.69	1.69
	2	1.27	1.50	1.50	1.51	1.52	1.52	1.53	1.53	1.54	1.54	1.55
	3	1.08	1.54	1.54	1.57	1.58	1.60	1.61	1.62	1.64	1.65	1.66
Median	1	1.54	1.73	1.73	1.74	1.75	1.75	1.76	1.76	1.68	1.78	1.78
	2	1.43	1.73	1.73	1.73	1.73	1.73	1.74	1.74	1.74	1.74	1.75
	3	1.07	1.72	1.72	1.72	1.72	1.72	1.72	1.73	1.73	1.73	1.73
SD	1	0.72	0.70	0.70	0.71	0.71	0.71	0.71	0.71	0.71	0.71	0.72
	2	0.78	0.80	0.80	0.80	0.80	0.80	0.81	0.81	0.81	0.81	0.81
	3	0.75	0.76	0.76	0.77	0.77	0.78	0.79	0.79	0.80	0.81	0.81
CV (%)	1	50.79	42.78	42.78	42.63	42.55	42.48	42.43	42.38	42.34	42.30	42.26
	2	61.41	53.06	53.06	52.92	52.85	52.79	52.73	52.68	52.62	52.57	52.53
	3	69.84	49.24	49.24	48.98	48.88	48.81	48.77	48.75	48.75	48.77	48.81

*P_n**—percentile of the *n* percentage, *SD*—standard deviation, *CV*—coefficient of variation

canopy height. This error for estimating plant height is associated with the influence of several factors, such as lodging plants that could compose a source of error for using high-resolution data. This condition is a common characteristic of pre-harvest condition, mainly due to the environmental factors (Canata et al. 2019; Cholula et al. 2020), and it was observed during the field measurements of the current study.

The lower RMSE (0.47 m) obtained for crop canopy height from Field 3 can be explained by the field condition and also by the capacity of the laser sensor to emit multiple pulses of signal and detecting the returns associated with the crop canopy (the highest data from point cloud). Harkel et al. (2020) reported similar results for modeling different crops (potato, sugar beet, and winter wheat) based on plant height indicated by laser sensor, they found RMSE values from 0.12 to 0.34 m, comparing manual plant height measurements and LiDAR data. The CHM generated to map the spatial variability of sugarcane fields is shown in Fig. 6a. The variation of the plant height indicated by the CHM would be a potential tool for detecting different levels of sugarcane production and, consequently, to help improve harvest planning and within-field management. Colaço et al. (2019) identified the spatial variability of orange orchards using TLS to provide site-specific management according to the height and volume of the plants.

The relationship between the observed and predicted crop height from CHM for each field (Field 1—Fig. 6B, Field 2—Fig. 6c, Field 3—Fig. 6d) showed that the accuracy (R^2) of the method ranged from 0.31 to 0.38, with the highest R^2 (0.38) for Field 3 considering both variables (stalk and canopy height). This effect can be associated with the maximum values considered for the interpolation used to generate DSM from the point cloud and to the structural condition of the plants at the field.

The descriptive statistics of LiDAR-derived metrics extracted from the point cloud is shown in Table 3 for the same validation points. These metrics can support preliminary filtering of the point cloud to eliminate signal noise and outliers from elevation data (Walter et al. 2019). The CV values ranged from 42 to 69% considering all fields, and the highest value was verified for P50th (69%—Field 3). This variation indicated a high level of spatial variability in sugarcane fields. The maximum values from percentiles P90th to P99th were similar to the maximum values of stalk height (2.70 m), indicating that extracting percentiles from point cloud would be a strategy to spatialize crop height without the influence of discrepant values. Overall, the CHM and the percentiles showed a systematic overestimation of the plant height that is partly affected by the spatial resolution compared to the size of the objects (plants), and the capacity to reconstruct the

canopy structure (Bareth et al. 2016; Holman et al. 2016). Other studies described the digital model applications for agriculture, Brocks and Bareth (2018) used digital models as a non-destructive method for monitoring the vegetative development of barley and for predicting dry matter biomass with high accuracy ($R^2 = 0.79$). Schirrmann et al. (2016) elaborated crop surface models for monitoring agronomic parameters of winter wheat using UAV imagery, which enabled them to detect the variations in early crop senescence and to model biophysical wheat parameters.

The relationship between the field measurements and the LiDAR data indicated the potential of RS tools to identify the spatial variability of sugarcane fields through the plant height mapping in the pre-harvest condition. This approach can provide relevant information to support site-specific management for sugarcane growers, and a suitable alternative to the multispectral information obtained during the crop maturation stage from aerial platforms. The economical and practical aspects also should be deeply discussed to enable the use of LiDAR-based platforms in the agricultural environment, considering that it tends to make feasible for long-term. As an alternative to minimize the measurement error of stalk height, future studies should develop the data filtering according to the returns of laser sensor to characterize better the structure of sugarcane plants.

Conclusion

The LiDAR-derived metrics associated with 3D sensing data processing were obtained to provide the characterization of the spatial variability of commercial sugarcane fields. The DTMs generated before and after harvesting were numerically the same regarding the elevation values, indicating that a single flight would be required to generate digital models in similar field conditions of the current study. The plant height distribution within-field was mapped through the CHM obtained from a dense point cloud. The RMSE was 0.47 m considering the comparison between the field measurements (sugarcane stalk height) and LiDAR data. LiDAR technology demonstrated potential to assess the spatial variability of sugarcane fields for the pre-harvest condition (crop maturation stage). The contribution of the technology to sugarcane industry involves large-scale crop mapping with more representative data previous harvesting.

Acknowledgements To the operational support of SAI Brazil and São Manoel sugarcane mill. This study was financed in part by the Coordenação de Aperfeiçoamento de Pessoal de Nível Superior—Brasil (CAPES)—Finance Code 001.

References

- Bareth, Georg, Juliane Bendig, Nora Tilly, Dirk Hoffmeister, Helge Aasen, and Andreas Bolten. 2016. A Comparison of UAV and TLS-derived Plant Height for Crop Monitoring: Using Polygon Grids for the Analysis of Crop Surface Models (CSMs). *Photogrammetrie, Fernerkundung, Geoinformation*. 2: 85–94. <https://doi.org/10.1127/pfg/2016/0289>.
- Bazewez, M.N., Y.A. Hussin, and E.H. Kloosterman. 2018. Integrating airborne LiDAR and terrestrial laser scanner forest parameters for accurate above-ground biomass/carbon estimation in Ayer Hitam tropical forest, Malaysia. *International Journal of Applied Earth Observation and Geoinformation* 73: 638–652. <https://doi.org/10.1016/j.jag.2018.07.026>.
- Bégué, Agnes, V. Lebourgeois, E. Bappel, P. Todoroff, A. Pellegrino, F. Baillarin, and B. Siegmund. 2010. Spatio-temporal variability of sugarcane fields and recommendations for yield forecast using NDVI. *International Journal of Remote Sensing* 31 (20): 5391–5407. <https://doi.org/10.1080/01431160903349057>.
- Brocks, Sebastian, and Georg Bareth. 2018. Estimating barley biomass with crop surface models from oblique RGB imagery. *Remote Sensing* 10 (2): 268. <https://doi.org/10.3390/rs10020268>.
- Buelvas, Roberto M., Viacheslav I. Adamchuk, Eko Leksono, Peter Tikasz, Mark Lefsrud, and Jarek Holoszkiwicz. 2019. Biomass estimation from canopy measurements for leafy vegetables based on ultrasonic and laser sensors. *Computers and Electronics in Agriculture* 164: 104896. <https://doi.org/10.1016/j.compag.2019.104896>.
- Canata, Tatiana Fernanda, José P. Molin, and Rafael Vieira de Sousa. 2019. A measurement system based on LiDAR technology to characterize the canopy of sugarcane plants. *Engenharia Agrícola* 39 (2): 240–247. <https://doi.org/10.1590/1809-4430-eng.agric.v39n2p240-247/2019>.
- Borra-Serrano, Irene, Tom De Swaef, Hilde Muylle, David Nuytens, Jürgen Vangeyte, Koen Mertens, Wouter Saeys, Ben Somers, Isabel Roldán-Ruiz, and Peter Lootens. 2019. Canopy height measurements and non-destructive biomass estimation of Lolium perenne swards using UAV imagery. *Grass Forage Science* 74: 356–369. <https://doi.org/10.1111/gfs.12439>.
- Cholula, Uriel, Jorge A. da Silva, Thiago Marconi, J Alex Thomason, J. Solorzano, and J. Enciso. 2020. Forecasting yield and lignocellulosic composition of energy cane using unmanned aerial systems. *Agronomy* 10 (5): 718. <https://doi.org/10.3390/agronomy10050718>.
- Mesas-Carrascosa, Francisco-Javier., Ana I. de Castro, Jorge Torres-Sánchez, Paula Triviño-Tarradas, Francisco M. Jiménez-Brenes, Alfonso García-Ferrer, and Francisca López-Granados. 2020. Classification of 3D Point Clouds Using Color Vegetation Indices for Precision Viticulture and Digitizing Applications. *Remote Sensing* 12: 317. <https://doi.org/10.3390/rs12020317>.
- Colaço, André Freitas., José Paulo. Molin, Joan R. Rosell-Polo, and Alexandre Escolà. 2018. Application of light detection and ranging and ultrasonic sensors to high-throughput phenotyping and precision horticulture: current status and challenges. *Horticulture Research* 5: 35. <https://doi.org/10.1038/s41438-018-0043-0>.
- Colaço, André Freitas., José Paulo. Molin, Joan R. Rosell-Polo, and Alexandre Escolà. 2019. Spatial variability in commercial orange groves. Part 1: canopy volume and height. *Precision Agriculture* 20: 788–804. <https://doi.org/10.1007/s11119-018-9612-3>.
- Silva, Carlos Alberto, Andrew Thomas Hudak, Carine Klauberg, Lee Alexandre Vierling, Carlos Gonzalez-Benecke, Samuel de Padua, Chaves Carvalho, Luiz Carlos Estraviz. Rodriguez, and

- Adrián Cardil. 2017. Combined effect of pulse density and grid cell size on predicting and mapping aboveground carbon in fast-growing Eucalyptus forest plantation using airborne LiDAR data. *Carbon Balance and Management* 12 (13): 1–16. <https://doi.org/10.1186/s13021-017-0081-1>.
- CONAB. Companhia Nacional de Abastecimento. <https://www.conab.gov.br/info-agro/safras/cana/boletim-da-safra-de-cana-de-acucar>
- da Cunha, Antonio Ribeiro, and Divaldo Martins. 2009. Classificação climática para os municípios de Botucatu e São Manuel, SP. *Irriga* 14 (1): 1–11. <https://doi.org/10.15809/irriga.2009v14n1p1-11>.
- Eitel, Jan, Troy S. Magney, Lee A. Vierling, Tabitha Brown, and David R. Huggins. 2014. LiDAR based biomass and crop nitrogen estimates for rapid, non-destructive assessment of wheat nitrogen status. *Field Crops Research* 159: 21–32. <https://doi.org/10.1016/j.fcr.2014.01.008>.
- Escolà, Alexandre, José A. Martínez-Casasnovas, Josep Rufat, Jaume Arnó, Amadeu Arbonés, Francesc Sebé, Miquel Pascual, Eduard Gregorio, and Joan R. Rosell-Polo. 2016. Mobile terrestrial laser scanner applications in precision friculture/horticulture and tools to extract information from canopy point clouds. *Precision Agriculture* 18: 111–132. <https://doi.org/10.1007/s11119-016-9474-5>.
- Li, Penglei, Xiao Zhang, Wenhui Wang, Hengbiao Zheng, Xia Yao, Yongchao Tian, Yan Zhu, Weixing Cao, Qi. Chen, and Tao Cheng. 2020. Estimating aboveground and organ biomass of plant canopies across the entire season of rice growth with terrestrial laser scanning. *International Journal of Applied Earth Observation and Geoinformation* 91: 102132. <https://doi.org/10.1016/j.jag.2020.102132>.
- Friedli, Michael, Norbert Kirchgessner, Christoph Grieder, Frank Liebisch, Michael Mannale, and Achim Walter. 2016. Terrestrial 3D laser scanning to track the increase in canopy height of both monocot and dicot crop species under field conditions. *Plant Methods*. <https://doi.org/10.1186/s13007-016-0109-7>.
- Gebredemhin, Alem, Pieter E. Badenhorst, Junping Wang, German C. Spangenberg, and Kevin F. Smith. 2019. Prospects for measurement of dry matter yield in forage breeding programs using sensor technologies. *Agronomy* 9 (2): 65. <https://doi.org/10.3390/agronomy9020065>.
- Luciano, Ana Cláudia, Michelle dos Santos, Cristina Araújo Picoli, Jansle Vieira Rocha, Henrique Coutinho Junqueira, Franco, Guilherme Martineli Sanches, Manoel Regis Lima Verde, Leal, and Guerric le Maire. 2018. Generalized space-time classifiers for monitoring sugarcane areas in Brazil. *Remote Sensing of Environment* 215: 438–451. <https://doi.org/10.1016/j.rse.2018.06.017>.
- Gomes, Frederico Pimentel, and Carlos Henrique Garcia. 2002. *Estatística aplicada a experimentos agrônomicos e florestais*. Piracicaba: FEALQ.
- Gorgens, Eric Bastos, Ruben Valbuena, and Luiz Carlos Estraviz. Rodriguez. 2017. A method for optimizing height threshold when computing airborne laser scanning metrics. *Photogrammetric Engineering & Remote Sensing* 83 (5): 343–350. <https://doi.org/10.14358/PERS.83.5.343>.
- Hämmerle, Martin, and Bernhard Höfle. 2014. Effects of reduced terrestrial LiDAR point density on high-resolution grain crop surface models in precision agriculture. *Sensors* 14 (12): 24212–24230. <https://doi.org/10.3390/s141224212>.
- ten Harkel, Jelle, Harm Bartholomeus, and Lammert Kooistra. 2020. Biomass and crop height estimation of different crops using UAV-based lidar. *Remote Sensing* 12 (1): 17. <https://doi.org/10.3390/rs12010017>.
- Holman, Fenner H., Andrew B. Riche, Adam Michalski, March Castle, Martin J. Wooster, and Malcolm J. Hawkesford. 2016. High throughput field phenotyping of wheat plant height and growth rate in field plot trials using UAV based remote sensing. *Remote Sensing* 8 (12): 1031. <https://doi.org/10.3390/rs8121031>.
- Hopkinson, Chris, Jenny Lovell, Laura Chasmer, David Jupp, Natascha Kljun, and Eva van Gorsel. 2013. Integrating terrestrial and airborne lidar to calibrate a 3D canopy model of effective leaf area index. *Remote Sensing of Environment* 136: 301–314. <https://doi.org/10.1016/j.rse.2013.05.012>.
- da Silva, Vanessa Sousa, C.A. Silva, M. Mohan, A. Cardil, F.E. Rex, G.H. Loureiro, D.R.A.D. Almeida, E.N. Broadbent, E.B. Gorgens, A.P. Dalla Corte, and E.A. Silva. 2020. Combined impact of sample size and modeling approaches for predicting stem volume in eucalyptus spp. forest plantations using field and LiDAR data. *Remote Sensing* 12 (9): 1438. <https://doi.org/10.3390/rs12091438>.
- Jiang, Yu., Changying Li, Fumiomi Takeda, Elizabeth A. Kramer, Hamid Ashrafi, and Jamal Hunter. 2019. 3D point cloud data to quantitatively characterize size and shape of shrub crops. *Horticulture Research*. <https://doi.org/10.1038/s41438-019-0123-9>.
- Jimenez-Berni, Jose A., Deery M. Deery, Pablo Rozas-Larraondo, Anthony Tony Condon, Greg J. Rebetzke, Richard A. James, William D. Bovill, Robert T. Furbank, and Xavier R. Sirault. 2018. High throughput determination of plant height, ground cover, and above-ground biomass in wheat with LiDAR. *Frontiers in Plant Science* 9: 237. <https://doi.org/10.3389/fpls.2018.00237>.
- Li, Wang, Zheng Niu, Hanyue Chen, and Dong Li. 2017. Characterizing canopy structural complexity for the estimation of maize LAI based on ALS data and UAV stereo images. *International Journal of Remote Sensing* 38 (8): 2106–2116. <https://doi.org/10.1080/01431161.2016.1235300>.
- Roussel, Jean-Romain, David Auty, Florian De Boissieu, Andrew Sánchez Meador. 2019. lidR: Airborne LiDAR data manipulation and visualization for forestry applications - version 2.0.2.
- Loudermilk, Louise E., J. Kevin Hiers, Joseph J. O'Brien, Robert J. Mitchell, Abhinav Singhania, Juan C. Fernandez, Wendell P. Cropper Jr, and K. Clint Slatton. 2009. Ground-based LiDAR: A novel approach to quantify fine-scale fuelbed characteristics. *International Journal of Wildland Fire* 18: 676–685. <https://doi.org/10.1071/WF07138>.
- Luo, Shezhou, Jing M. Chen, Cheng Wang, Xiaohuan Xi, Hongcheng Zeng, Dailiang Peng, and Dong Li. 2016. Effects of LiDAR point density, sampling size and height threshold on estimation accuracy of crop biophysical parameters. *Optics Express* 24 (11): 11578–11593. <https://doi.org/10.1364/OE.24.011578>.
- Maes, Wouter H., and Kathy Steppe. 2019. Perspectives for remote sensing with unmanned aerial vehicles in precision agriculture. *Trends in Plant Science* 24 (2): 152–164. <https://doi.org/10.1016/j.tplants.2018.11.007>.
- Maimaitijiang, Maitiniyazi, Vasit Sagan, Paheding Sidike, Sean Hartling, Flavio Esposito, and Felix B. Fritsch. 2020. Soybean yield prediction from UAV using multimodal data fusion and deep learning. *Remote Sensing of Environment*. <https://doi.org/10.1016/j.rse.2019.111599>.
- Wang, Ming, Zhengjia Liu, Muhammad Hasan Ali, Baig, Yongsheng Wang, Yurui Li, and Yuanyan Chen. 2019. Mapping sugarcane in complex landscapes by integrating multi-temporal Sentinel-2 images and machine learning algorithms. *Land Use Policy* 88: 104190. <https://doi.org/10.1016/j.landusepol.2019.104190>.
- Mielcarek, Mi.łosż, Krzysztof Stereńczak, and Anahita Khosravipour. 2018. Testing and evaluating different LiDAR-derived canopy height model generation methods for tree height estimation. *International Journal of Applied Earth Observation and Geoinformation* 71: 132–143. <https://doi.org/10.1016/j.jag.2018.05.002>.

- Mielcarek, Milosz, Agnieszka Kamińska, and Krzysztof Stereńczak. 2020. Digital aerial photogrammetry (DAP) and airborne laser scanning (ALS) as sources of information about tree height: Comparisons of the accuracy of remote sensing methods for tree height estimation. *Remote Sensing* 12 (11): 1808. <https://doi.org/10.3390/rs12111808>.
- Molijn, Ramses A., Lorenzo Iannini, Jansle Vieira Rocha, and Ramon F. Hanssen. 2018. Ground reference data for sugarcane biomass estimation in São Paulo state, Brazil. *Science Data* 5 (180150): 1–18. <https://doi.org/10.1038/sdata.2018.150>.
- Molin, José Paulo., André Freitas. Colaço, and Amaral do Lucas Rios . 2015. *Agricultura de precisão*, 1st ed. Piracicaba: Oficina de Textos.
- Tilly, Nora, Dirk Hoffmeister, Qiang Cao, Shanyu Huang, Victoria Lenz-Wiedemann, Yuxin Miao, and Georg Bareth. 2014. Multitemporal crop surface models: accurate plant height measurement and biomass estimation with terrestrial laser scanning in paddy rice. *Journal of Applied Remote Sensing* 8 (1): 083671. <https://doi.org/10.1117/1.JRS.8.083671>.
- Murray, Jon, Joseph T. Fennell, George Alan Blackburn, James Duncan Whyatt, and Bo. Li. 2020. The novel use of proximal photogrammetry and terrestrial LiDAR to quantify the structural complexity of orchard trees. *Precision Agriculture* 21: 473–483. <https://doi.org/10.1007/s11119-019-09676-4>.
- Okrimenko, Maxim, Craig Coburn, and Chris Hopkinson. 2019. Multi-spectral lidar: Radiometric calibration, canopy spectral reflectance, and vegetation vertical SVI profiles. *Remote Sensing* 11 (13): 1556. <https://doi.org/10.3390/rs11131556>.
- Paulus, Stefan, Jan Behmann, Anne-Katrin. Mahlein, Lutz Plümer, and Heiner Kuhlmann. 2014. Low-cost 3D systems - well suited tools for plant phenotyping. *Sensors* 14 (2): 3001–3018. <https://doi.org/10.3390/s14020300>.
- Paulus, Stefan. 2019. Measuring crops in 3D: Using geometry for plant phenotyping. *Plant Methods* 15: 103. <https://doi.org/10.1186/s13007-019-0490-0>.
- Poley, Lucy G., and Gregory J. McDermid. 2020. A systematic review of the factors influencing the estimation of vegetation aboveground biomass using unmanned aerial systems. *Remote Sensing* 12 (7): 1052. <https://doi.org/10.3390/rs12071052>.
- Portz, Gustavo, José Paulo. Molin, and J. Jasper. 2012. Active crop sensor to detect variability of nitrogen supply and biomass on sugarcane fields. *Precision Agriculture*. <https://doi.org/10.1007/s11119-011-9243-4>.
- Deery, David, Jose Jimenez-Berni, Hamlyn Jones, Xavier Sirault, and Robert Furbank. 2014. Proximal remote sensing buggies and potential applications for field-based phenotyping. *Agronomy* 4 (3): 349–379. <https://doi.org/10.3390/agronomy4030349>.
- QGIS Development Team. 2018. QGIS geographic information system. Open-source geospatial foundation project.
- R Core Team. R. 2018. A language and environment for statistical computing. R Foundation for Statistical Computing: Vienna, Austria.
- Rahman, Muhammad Moshir, and Andrew Robson. 2020. Integrating landsat-8 and sentinel-2 time series data for yield prediction of sugarcane crops at the block level. *Remote Sensing* 12 (8): 1313. <https://doi.org/10.3390/rs12081313>.
- Gené-Mola, Jordi, Eduard Gregorio, Fernando Auat Cheein, Javier Guevara, Jordi Llorens, Ricardo Sanz-Cortiella, Alexandre Escolà, and Joan R. Rosell-Polo. 2020. Fruit detection, yield prediction and canopy geometric characterization using LiDAR with forced air flow. *Computers and Electronics in Agriculture* 168: 105121. <https://doi.org/10.1016/j.compag.2019.105121>.
- Ross, Nelson. 2013. How did we get here? An early history of forestry lidar. *Canadian Journal of Remote Sensing* 39 (1): 6–17. <https://doi.org/10.5589/m13-011>.
- Saiz-Rubio, Verónica, and Francisco Rovira-Más. 2020. From smart farming towards agriculture 5.0: A review on crop data management. *Agronomy Journal* 10 (2): 207. <https://doi.org/10.3390/agronomy10020207>.
- Schirrmann, Michael, Antje Giebel, Franziska Gleiniger, Michael Pflanz, Jan Lentschke, and Karl-Heinz. Dammer. 2016. Monitoring agronomic parameters of winter wheat crops with low-cost UAV imagery. *Remote Sensing* 8 (9): 706. <https://doi.org/10.3390/rs8090706>.
- Shendryk, Yuri, Jeremy Sofonia, Robert Garrard, Yannik Rist, Danielle Skocaj, and Peter Thorburn. 2020. Fine-scale prediction of biomass and leaf nitrogen content in sugarcane using UAV LiDAR and multispectral imaging. *International Journal of Applied Earth Observation and Geoinformation* 92: 102177. <https://doi.org/10.1016/j.jag.2020.102177>.
- Sun, Shangpeng, Changying Li, Andrew H. Paterson, Yu. Jiang, Xu. Rui, Jon S. Robertson, John L. Snider, and Peng W. Chee. 2018. In-field high throughput phenotyping and cotton plant growth analysis using LiDAR. *Frontiers in Plant Science*. <https://doi.org/10.3389/fpls.2018.00016>.
- Tilly, Nora, Helge Aasen, and George Bareth. 2015. Fusion of plant height and vegetation indices for the estimation of barley biomass. *Remote Sensing* 7 (12): 11449–11480. <https://doi.org/10.3390/rs70911449>.
- Walter, James D. C., James Edwards, Glenn McDonald, and Haydn Kuchel. 2019. Estimating biomass and canopy height with LiDAR for field crop breeding. *Frontiers in Plant Science* 10: 1145. <https://doi.org/10.3389/fpls.2019.01145>.

Publisher's Note Springer Nature remains neutral with regard to jurisdictional claims in published maps and institutional affiliations.